CHINESE OPTICS LETTERS

Vol. 19, No. 12 | December 2021

Non-mechanical beam scanner based on VCSEL integrated amplifier with resonant wavelength detuning design

Shanting Hu (胡善亭)[1,2*], Xiaodong Gu (顾晓东)[2,3], Masanori Nakahama (中滨正统)[2,3], and Fumio Koyama (小山二三夫)[2]

[1] Beijing University of Posts and Telecommunications, Beijing 100876, China

[2] Institute of Innovative Research (IIR), Tokyo Institute of Technology, 4259-R2-22 Nagatsuta-cho, Midori-ku, Yokohama 226-8503, Japan

[3] Ambition Photonics Inc., Yokohama 226-8510, Japan

*Corresponding author: hu.s.ab@m.titech.ac.jp

Received April 12, 2021 | Accepted June 4, 2021 | Posted Online September 15, 2021

We demonstrate the non-mechanical beam steering and amplifier operation of a vertical cavity surface emitting laser (VCSEL) integrated Bragg reflector waveguide amplifier with a cut-off wavelength detuning design, which enables unidirectional lateral coupling, continuous electrical beam steering, and diffraction-limited divergence angle. We present the modeling of the proposed structure for unidirectional coupling between a seed single-mode VCSEL and slow-light amplifier. We also present the detailed operating characteristics including the near-field and far-field patterns, light/current characteristics, and lasing spectrum. The experimental measurements exhibit a single-mode output of over 8 mW under CW operation, a continuous beam steering range of 16°, and beam divergence below 0.1° as an optical beam scanner. The integrated amplifier length is as small as 0.9 mm, and thus we could expect much higher powers and higher resolution points by increasing the amplifier lengths.

Keywords: VCSEL integrated amplifier; unidirectional coupling; optical beam scanner.

DOI: 10.3788/COL202119.121403

1. Introduction

As for applications such as 3D scanners, LiDAR, and free-space optical communications, optical scanning technology with low cost, high resolution, and high speed is highly demanded[1–6]. While a mechanical beam scanner has been commercially available, there remain difficulties such as its large module size, uncertain long-term reliability, and low steering speed. With the potential of low cost and super compactness, solid-state scanning is considered to be an attractive option. On the other hand, vertical cavity surface emitting lasers (VCSELs) have various advantages such as low cost, high efficiency, and ease for mass production[7–11]. Solid-state scanning devices utilizing a two-dimensional (2D) VCSEL array and phased arrays have been reported, but there still remain difficulties in their limited steering performances[12–16].

In our group, a solid-state scanner based on a VCSEL structure is proposed and demonstrated[17–19]. In the device, an input light from a tunable laser is coupled into the Bragg reflector waveguide by a lensed fiber. When the waveguide is pumped above threshold, amplification of the coupling light along the waveguide can be achieved. The amplified output gets larger and larger by increasing the device length, and the corresponding beam divergence becomes smaller and smaller. Large angle beam steering can be achieved by a scan through the input wavelength since the slow-light waveguide can provide large dispersion near the cut-off wavelength. We then presented a 10 mW class single-mode amplifier composed of a VCSEL working as a seed laser laterally integrated with a slow-light waveguide[20,21]. However, when we pump the seed laser and the slow-light waveguide (amplifier) simultaneously, the coupling light from the slow-light waveguide functioning as a multi-mode VCSEL will cause mode hopping and multi-mode operation in the seed laser. Mutual coupling between the seed laser and amplifier strictly limits the beam steering range of the device, since the beam steering range is dependent on the continuous wavelength tuning range of the seed laser.

In this paper, we demonstrate a novel beam scanner based on a VCSEL integrated amplifier with an in-plane cut-off wavelength detuning design. Thanks to the mode stability brought by the unidirectional behavior of the new structure, a continuous beam steering of 16° is obtained, exhibiting a record number of resolution points of over 200 for the total chip length of 1.2 mm, which has been a great improvement compared with our former work in Ref. [21], which exhibits 13° beam steering range and 30 resolution points.

2. Structure and Modeling

The schematic illustration of our solid-state VCSEL beam scanner is shown in Fig. 1. The half-VCSEL structure is that of conventional 850 nm VCSELs without a top distributed Bragg reflector (DBR). The device has the same vertical structure as that of a half-VCSEL with four pairs of AlGaAs top DBRs and a phase control layer, which includes two sections integrated laterally: one VCSEL on the left and a long VCSEL amplifier on the right side. The amplifier section can also act as a multi-mode VCSEL when pumped above the threshold. The two sections are electrically isolated via an ion implantation process. The phase control layer on top of the VCSEL section is partly removed by wet-etching to form a resonant wavelength separation between the two sections. Then, a seven-pair SiO_2/Ta_2O_5 dielectric mirror is deposited as the top DBR to acquire high reflectivity for lasing[22,23]. As shown in Fig. 1(b), due to wet-etching of the phase control layer, the cavity resonance of the VCSEL shifts to a shorter wavelength[24,25]. Thereafter, unidirectional coupling behavior can be achieved in the new structure, since a longer wavelength light in the amplifier section cannot be coupled to the VCSEL section due to its cut-off condition, as stated in Refs. [26–28].

Figure 1(c) shows the top view of a fabricated device, where the oxidized aperture of a VCSEL section is 3 μm × 3 μm, and the length of an amplifier section is 900 μm. A 150 μm long unpumped taper section is also formed to avoid the reflection at the end of the amplifier. The total chip length is 1.2 mm.

The amount of wavelength detuning is calculated by utilizing a standard transfer matrix method[29–31]. The modeling is based on a structure of an 850 nm half-VCSEL composed of four-pair AlGaAs top DBR and 40-pair bottom DBR. The calculated transmittances in each cavity are shown in Fig. 2(a). Detuning of 7 nm of the lasing wavelength of the seed laser from that of the amplifier can be achieved when the phase control layer of the seed laser is removed by 30 nm through wet-etching.

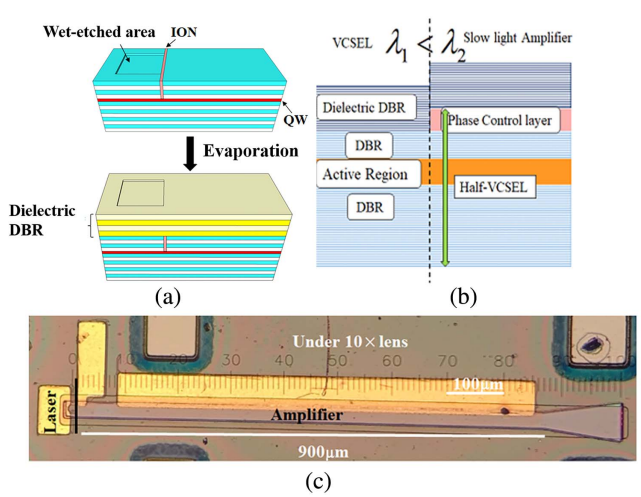

Fig. 1. Schematic of the proposed solid-state beam scanner from the (a) side view and (b) cross-sectional view; (c) top view of a fabricated beam scanner.

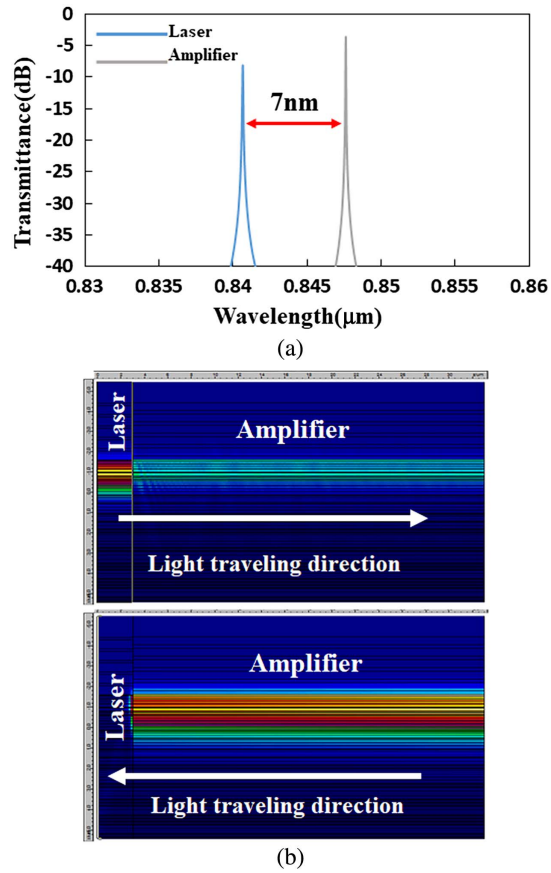

Fig. 2. (a) Transmittance of top DBR mirror of the VCSEL seed laser section and amplifier section when 30 nm of the phase control layer of the VCSEL side is removed as a function of wavelength; (b) simulation results of lateral coupling behavior when the seed laser and amplifier are pumped separately.

Figure 2(b) shows the simulation results of the unidirectional coupling utilizing the film mode matching method[32]. We use a parameter coupling efficiency η to evaluate the coupling strength between the two cavities. η is defined in the following equation:

$$\eta = \frac{\alpha_c}{\alpha_a + \alpha_m + \alpha_c}, \tag{1}$$

where α_c is the coupled rate per unit length for lateral coupling light, α_m is the radiation loss per unit length for vertical emission light through a top mirror, and α_a is the loss per unit length for the absorption loss in the cavity.

α_c is calculated through the following equation:

$$\alpha_c = \frac{\int |E_o|^2 \mathrm{d}y \cdot v_g}{\iint_{\mathrm{vcsel}} |E|^2 \mathrm{d}y\mathrm{d}z}, \tag{2}$$

where v_g is the group velocity of the slow-light mode, E_o is the electric-field distribution in the coupled cavity waveguide, and E is the electric-field distribution in the lasing VCSEL cavity. It is similar to the definition of the slope efficiency of edge emitting lasers.

When a slow-light mode at the wavelength in the VCSEL cavity (840 nm) is excited, a large amount of power is coupled into the amplifier section. The coupling efficiency is as large as 70%. However, when we assumed a slow-light mode excited in the amplifier section, which is 0.5 nm shorter than the vertical resonant wavelength (847 nm), the lateral leakage of light from the amplifier section to the seed VCSEL can barely be seen. The coupling efficiency is less than 0.1%, which is limited by the calculation accuracy. The unidirectional coupling behavior of our proposed VCSEL integrated amplifier helps us to realize stable lateral coupling.

3. Experimental Results and Discussions

The measured lasing spectra for the VCSEL and amplifier sections pumped separately when the phase layer on top of the VCSEL is partly removed by wet-etching are shown in Fig. 3(a), which has the same structure as we assumed in the simulation. As can be seen, when 30 nm of the phase layer on top of the VCSEL section is wet-etched, the lasing wavelength of the amplifier (843.5 nm) is around 7.5 nm longer than that of the seed VCSEL (837 nm). Good agreement is shown between the simulation and experimental results. The near-field pattern (NFP) is shown in Fig. 3(b) when we pump the VCSEL and amplifier section separately. As shown in Fig. 3(b), the strong leakage light from the VCSEL into the amplifier section can be seen in the NFP when we only pump the seed VCSEL section, which indicates strong coupling from the seed VCSEL into the amplifier. At the same time, hardly any coupling can be seen from the reverse direction when we only pump the amplifier, as shown in the bottom figure. The unidirectional coupling behavior we observed in the experiment agrees well with the simulation results, as demonstrated in Fig. 2(b). We could estimate the coupled slow-light power from the VCSEL to the amplifier through calculating the absorbed power in the amplifier section when the amplifier section is reversely biased, which is similar to the situation in the electro-absorption waveguide modulator[33]. Figure 3(c) shows the measured photocurrent with a reverse bias voltage at the amplifier section and a current pump of 8 mA at the VCSEL. A maximum photocurrent of 0.5 mA is obtained with a reversed voltage of −2 V at the amplifier, which corresponds to an absorbed power around 0.6 mW.

We show the amplifier function and beam steering performance of the 850 nm VCSEL integrated with a 900 μm amplifier/beam scanner. When a slow light is coupled from the VCSEL, the coupled slow light is amplified in the amplifier pumped above the threshold current. The measured far-field pattern (FFP) when two sections are pumped simultaneously is presented in Fig. 4(a), showing a narrow single peak at a deflection angle of 19.5°. When the VCSEL is pumped at 8 mA and the amplifier is pumped at 100 mA CW current, a single-peak FFP with a diffraction-limited narrow beam divergence of 0.06° can be seen. It is close to the calculated diffraction limit of 0.04° for a 900 μm long amplifier. The measurment result of light/current (L/I) as a function of the amplifier current

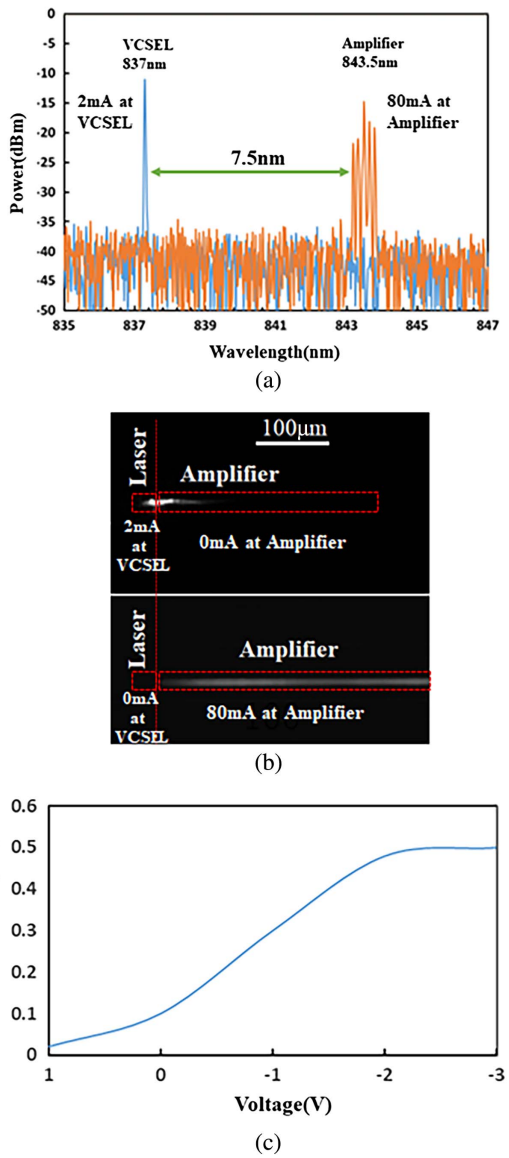

Fig. 3. (a) Measured spectrum of the VCSEL seed laser and amplifier pumped separately when 30 nm of the phase control layer of VCSEL side is removed; (b) experimentally measured NFP when the VCSEL seed laser and amplifier are pumped separately; (c) photocurrent against reversed voltage at the amplifier.

with 8 mA current pump at the VCSEL is shown in Fig. 4(b). The output power is limited by the coupled power from the seed VCSEL. Very recently, we proposed a surface grating loaded seed VCSEL, which can offer larger coupling power. An output power could be over 1 W. The result will be reported elsewhere. A large area photo-detector is put above the device with a tilted angle of 25° to avoid capturing the vertical emission power. An output power of over 8 mW was obtained. Single-mode operation can be confirmed in the spectrum, as shown in Fig. 4(c). Single-mode lasing at the wavelength of the seed VCSEL with side-mode suppression ratio (SMSR) of over 25 dB can be witnessed in the entire current range. Compared with the former

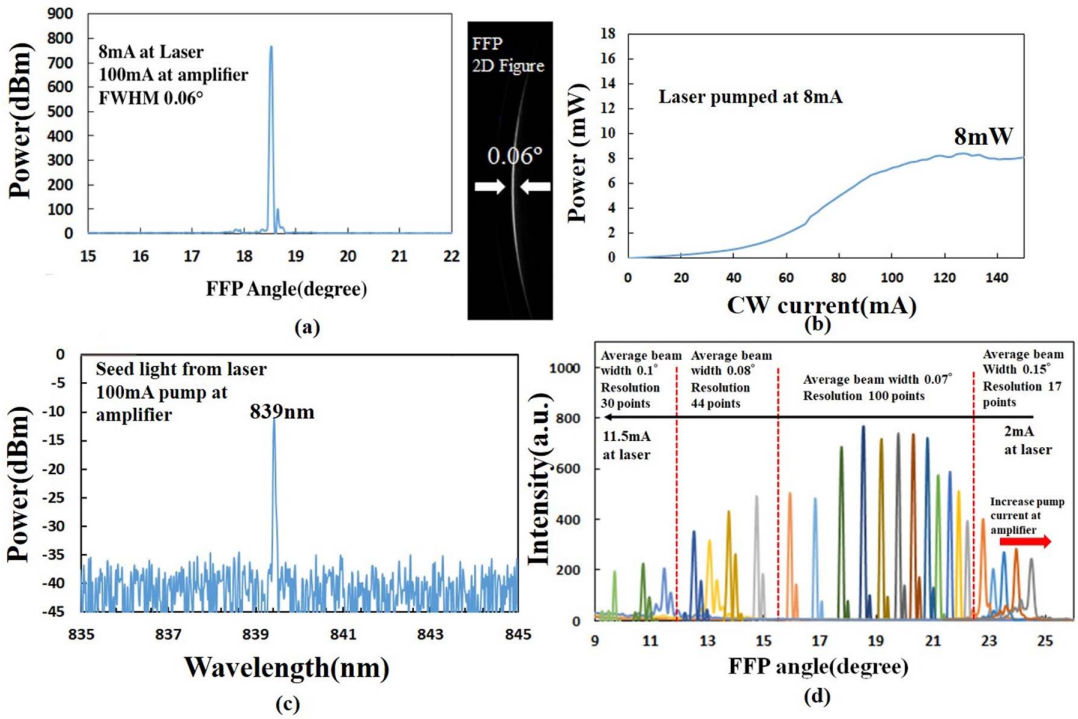

Fig. 4. (a) Measured FFP of amplified slow light; (b) output power of the device under amplification against the pump current at the amplifier; (c) measured lasing spectrum of the amplifier with the current pump; (d) continuous beam steering through push–pull current pumping.

result of the amplified lasing spectrum in Ref. [20], Fig. 4(c) clearly shows that the single-mode stability of our new device is improved thanks to the unidirectional behavior brought by the resonant wavelength detuning design.

Continuous beam steering is carried out by changing the injection current of the seed VCSEL, as shown in Fig. 4(d). The lasing wavelength of the seed VCSEL can be electro-thermally tuned continuously due to the self-heating effect[34,35]. A continuous change in the injection current of the seed VCSEL leads to a continuous sweep of the beam deflection angle from the amplifier. At the same time, when we change the pump current in the amplifier, the refractive index of the amplifier will also increase due to self-heating. As a result, the FFP angle will increase when we increase the pump current, which provides the push–pull operation for beam steering[36]. A beam divergence is dependent on the injection current with the narrowest divergence of around 0.06°. A total scanning range of 16° under the push–pull pumping is achieved with a resolution of 200 points, which is a record high resolution for a non-mechanical beam scanner with an integrated light souce. The side lobe of FFP in Figs. 4(a) and 4(d) could be due to the non-uniform current distribution in the amplifier, which is caused by a single-probe measurement in the experiment. This could be improved by wire-bonding for better current uniformity.

We also carried out the measurement of the beam steering speed of the integrated device. By applying a sinusoidal modulation current at the seed VCSEL, we are able to measure the dynamic response of the beam steering. Figure 5(a) shows the measured FFP with different modulation frequencies of the

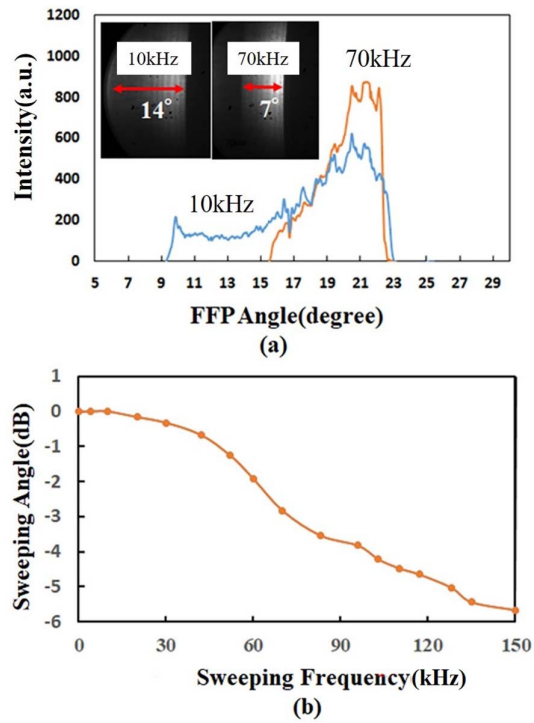

Fig. 5. (a) Averaged FFP of the device when the VCSEL side is pumped by a sinusoidal modulation current with modulation frequencies of 70 kHz and 10 kHz; (b) dynamic response of the beam steering.

sinusoidal current. Since the capture time of the FFP camera is much slower than the modulation frequency of the beam steering, the data show the averaged FFP. The full width of the averaged FFP is shown as a function of the modulation frequency in Fig. 5(b). The beam steering angle decreases as the modulation frequency increases. The 3 dB bandwidth of beam steering is over 70 kHz, which is much larger than that of mechanical beam steering devices. It could be large enough for beam scanning LiDAR with a typical frame rate of 30–50 frames per second.

4. Conclusion

The novel concept of the lateral integration of a VCSEL and amplifier with unidirectional coupling is given for non-mechanical beam scanners. The simulation and experimental measurements of a VCSEL integrated non-mechanical beam scanner with an amplifier function are demonstrated. We carried out the design of a slow-light amplifier laterally integrated with a VCSEL, which avoids mutual lateral coupling due to the in-plane resonant wavelength detuning. We also experimentally showed that slow light is coupled unidirectionally from the VCSEL to the amplifier. Beam steering is able to be achieved by simply changing the injection current at the VCSEL. The device shows a single-mode power of over 8 mW for VCSELs thanks to the amplifier integration.

We achieved a continuous beam steering range of 16°, beam divergence below 0.1°, and, hence, a record number of resolution points of over 200 for a solid-state beam scanner with the integration of a light source. After optimization of the designs and fabrication processes, further enhancement of the pulsed single-mode power up to 1 W is expected by extending the length of amplifier to several millimeters (mm) since we confirmed the output power is in proportion to the amplifier length. Also, the number of resolution points could be improved at the same time. Although we only demonstrated the one-dimensional (1D) beam steering of our device in this paper, 2D beam steering[37] can also be achieved through fabricating a 1D array of our proposed device and adding a cylindrical lens to the system. Our integrated solid-state scanner is promising as a key component in VCSEL photonics, providing a powerful engine for various applications such as 3D camera and LiDAR thanks to its compact and non-mechanical fashion.

Acknowledgement

This work was supported by JST ACCEL.

References

1. P. Varatharajah, A. B. Aceves, and J. V. Moloney, "All-optical spatial scanner," Appl. Phys. Lett. **54**, 2631 (1989).
2. Z. Yaqoob, A. A. Rizvi, and N. A. Riza, "Free-space wavelength-multiplexed optical scanner," Appl. Opt. **40**, 6425 (2001).
3. K. Moriki, Y. Ohnishi, H. Uchida, T. Hattori, and K. Iga, "Optical beam scanner with phase-variable semiconductor waveguides," Jpn. J. Appl. Phys. **29**, 1276 (1990).
4. W. Jun, D. T. McCormick, J. Zhang, L. Wang, N. C. Tien, and Z. Chen, "Three-dimensional endoscopic optical coherence tomography by use of a two-axis microelectromechanical scanning mirror," Appl. Phys. Lett. **88**, 163901 (2006).
5. J. Yun, C. Gao, S. Zhu, C. Sun, H. He, L. Feng, L. Dong, and L. Niu, "High-peak-power, single-mode, nanosecond pulsed, all-fiber laser for high resolution 3D imaging LIDAR system," Chin. Opt. Lett. **10**, 121402 (2012).
6. K. Scholle, E. Heumann, and G. Huber, "Single mode Tm and Tm, Ho:LuAG lasers for LIDAR applications," Laser Phys. Lett. **1**, 285 (2004).
7. M. A. Taubenblatt, "Optical interconnects for high-performance computing," J. Lightwave Technol. **30**, 448 (2012).
8. F. Koyama, "Recent advances of VCSEL photonics," J. Lightwave Technol. **24**, 4502 (2006).
9. K. Iga, "Forty years of vertical-cavity surface-emitting laser: invention and innovation," Jpn. J. Appl. Phys. **57**, 08PA01 (2018).
10. H. Kosaka, Jpn. J. Appl. Phys. **37**, 1394 (1998).
11. P. Guo, C. Zhang, J. Li, W. Yang, D. Parekh, C. J. Chang-Hasnain, W Hu, A. Xu, and Z. Chen, "Long distance transmission of SC-FDMA signals by directly-modulated OIL-VCSEL," Chin. Opt. Lett. **10**, 091407 (2012).
12. A. C. Lehman, D. F. Siriani, and K. D. Choquette, "Two-dimensional electronic beam-steering with implant-defined coherent VCSEL arrays," Electron. Lett. **43**, 22 (2007).
13. M. T. Johnsona, D. F. Sirianib, M. P. Tanc, and K. D. Choquette, "Beam steering via resonance detuning in coherently coupled vertical cavity laser arrays," Appl. Phys. Lett. **103**, 201115 (2013).
14. D. F. Siriani and K. D. Choquette, "Electronically controlled two-dimensional steering of in-phase coherently coupled vertical-cavity laser arrays," IEEE Photon. Technol. Lett. **23**, 167 (2011).
15. K. V. Acoleyen, W. Bogaerts, and R. Baets, "Two-dimensional optical phased array antenna on silicon-on-insulator," Opt. Express **18**, 13655 (2010).
16. J. Doylend, M. Heck, J. Bovington, J. Peters, L. Coldren, and J. Bowers, "Two-dimensional free-space beam steering with an optical phased array on silicon-on-insulator," Opt. Express **19**, 21595 (2011).
17. M. Nakahama, X. Gu, A. Matsutani, T. Sakaguchi, and F. Koyama, "Slow light VCSEL amplifier for high-resolution beam steering and high-power operations," in *CLEO* (2016), paper SF1L.5.
18. M. Morinaga, X. Gu, K. Shimura, M. Nakahama, A. Matsutani, and F. Koyama, "VCSEL amplifier with high power and narrow divergence applying a folded waveguide layout," in *CLEO* (2018), paper JTu2A.11.
19. Z. Ho, K. Shimura, X. Gu, M. Nakahama, A. Matsutani, and F. Koyama, "High-resolution beam steering of slow light VCSEL amplifier," in *CLEO-PR* (2017), p. 1.
20. X. Gu, M. Nakahama, A. Matsutani, and F. Koyama, "VCSEL-integrated Bragg reflector waveguide amplifier with single-mode output power over 10 mW," in *OECC* (2016), p. 1.
21. K. Shimura, Z. Ho, M. Nakahama, X. Gu, A. Matsutani, and F. Koyama, "Non-mechanical beam scanner integrated VCSEL for solid state LiDAR," in *CLEO-PR* (2017), paper s2566.
22. T. Tawara, H. Gotoh, T. Akasaka, N. Kobayashi, and T. Saitoh, "Low-threshold lasing of InGaN vertical-cavity surface-emitting lasers with dielectric distributed Bragg reflectors," Appl. Phys. Lett. **83**, 830 (2003).
23. D. Sun, F. Wenjun, P. Kner, J. Boucart, T. Kageyama, R. Pathak, D. Zhang, and W. Yuen, "Sub-mA threshold 1.5-μm VCSELs with epitaxial and dielectric DBR mirrors," IEEE Photon. Technol. Lett. **15**, 1677 (2003).
24. G. R. Hadley, "Effective index model for vertical-cavity surface-emitting lasers," Opt. Lett. **20**, 1483 (1995).
25. C. J. Chang-Hasnain, "Tunable VCSEL," IEEE J. Sel. Top. Quantum. Electron. **6**, 978 (2000).
26. S. T. Hu, A. Matsutani, and F. Koyama, "Unidirectional coupling of laterally coupled VCSEL and slow light modulator/amplifier," in *CLEO-PR* (2017), paper s2579.
27. S. T. Hu, M. Takanohashi, X. D. Gu, A. Matsutani, and F. Koyama, "Lateral integration of VCSEL and amplifier with resonant wavelength detuning design," IEICE Electron. Express **17**, 20190688 (2020).
28. S. T. Hu, M. Takanohashi, X. D. Gu, K. Shimura, and F. Koyama, "Lateral integration of VCSEL and amplifier with resonant wavelength detuning design," in *CLEO_SI* (2019), paper SM4N.3.
29. C. W. Tee, C. C. Tan, and S. F. Yu, "Design of antiresonant-reflecting optical waveguide-type vertical-cavity surface-emitting lasers using transfer matrix method," IEEE Photon. Technol. Lett. **15**, 1231 (2003).

30. W. Gang, L. Bin, P. Wei, and X. Jie, "A transfer matrix-based analysis of vertical-cavity semiconductor optical amplifiers," Chin. Phys. Lett. **22**, 2561 (2005).
31. G. R. Hadley, K. L. Lear, M. E. Warren, K. D. Choquette, J. W. Scott, and S. W. Corzine, "Comprehensive numerical modeling of vertical-cavity surface-emitting lasers," IEEE J. Quantum Electron. **32**, 607 (1996).
32. K. Yasuura, K. Shimohara, and T. Miyamoto, "Comprehensive numerical modeling of vertical-cavity surface-emitting lasers," J. Opt. Soc. Am. **70**, 183 (1980).
33. G. L. Li, R. B. Welstand, W. X. Chen, J. T. Zhu, S. A. Pappert, C. K. Sun, Y. Z. Liu, and P. K. L. Yu, "Novel bias control of electroabsorption waveguide modulator," IEEE Photon. Technol. Lett. **10**, 672 (1998).
34. F. Koyama, T. Mukaihara, Y. Hayashi, N. Ohnoki, N. Hatori, and K. Iga, "Wavelength control of vertical cavity surface-emitting lasers by using non-planar MOCVD," IEEE Photon. Technol. Lett. **7**, 10 (1995).
35. J. Chen, A. Hangauer, and M. C. Amann, "Simplified model of the dynamic thermal tuning behavior of VCSELs," IEEE Photon. Technol. Lett. **20**, 1082 (2008).
36. X. Gu, T. Shimada, A. Fuchida, A. Matsutani, A. Imaura, and F. Koyama, "Beam steering in GaInAs/GaAs slow-light Bragg reflector waveguide amplifier," Appl. Phys. Lett. **99**, 211107 (2011).
37. S. R. Davis, G. Farca, S. D. Rommel, S. Johnson, and M. H. Anderson, "Liquid crystal waveguides: new devices enabled by >1000 waves of optical phase control," Proc. SPIE **7618**, 76180E (2010).